



Contents lists available at ScienceDirect

## International Dairy Journal

journal homepage: [www.elsevier.com/locate/idairyj](http://www.elsevier.com/locate/idairyj)

## Heat stability of whey protein ingredients based on state diagrams

Rini Triani<sup>1</sup>, E. Allen Foegeding\*

Department of Food, Bioprocessing and Nutrition Sciences, North Carolina State University, Raleigh, NC, 27695, USA



## ARTICLE INFO

## Article history:

Received 2 October 2018  
 Received in revised form  
 3 December 2018  
 Accepted 4 December 2018  
 Available online 2 January 2019

## ABSTRACT

A state diagram approach was used to compare heat stability among whey protein ingredients. Solutions were thermal processed and solubility, turbidity, and colloidal structure (sol, precipitate, or gel) were plotted against the variables of pH (3–7) and protein concentration (1–10%, w/w) to form state diagrams. Each of the whey protein ingredients produced state diagrams with unique patterns in the protein concentrations associated with colloidal structures and in heat stability regions. Relative heat stability among ingredients depended on the pH-thermal processing combination, in that patterns observed at  $\text{pH} \leq 4.5$  were not equivalent to patterns produced at  $\text{pH} > 4.5$ . Heating at temperatures of  $< 100^\circ\text{C}$  for extended time did not produce the same results as heating at  $> 100^\circ\text{C}$  for short times. State diagrams were able to differentiate among the whey protein ingredients, but absolute values were determined by the heating treatment.

© 2019 Elsevier Ltd. All rights reserved.

## 1. Introduction

Consumers are increasingly aware of the benefits of protein for human health and specifically whey proteins. The health goals are commonly directed toward muscle maintenance, satiety, and weight management (Ha & Zemel, 2003; Hulmi et al., 2015; Katsanos et al., 2008; Luhovyy, Akhavan, & Anderson, 2007; Paddon-Jones et al., 2015; Phillips, Chevalier, & Leidy, 2016). The nutritional quality of whey protein comes in part from its high content of branched chain amino acids (Blomstrand, Eliasson, Karlsson, & Kohnke, 2006; Hoffman & Falvo, 2004; Kimball & Jefferson, 2006). Whey proteins can provide other health benefits, including lowering blood pressure, blood sugar, and reducing symptoms of stress and depression (Jakubowicz & Froy, 2013; Kawase, Hashimoto, Hosoda, Morita, & Hosono, 2000; Markus et al., 2000; Pal & Ellis, 2010). This has led to a desire to increase the content of whey protein in a variety of foods.

Whey protein ingredients are made by a series of processing unit operations that remove water, lactose, minerals, and lipid. The two most common forms of whey protein ingredients are whey protein concentrate (WPC; containing 25–80% protein) and whey

protein isolates (WPI; containing  $\geq 90\%$  protein) (Foegeding, Luck, & Vardhanabhuti, 2011). The WPC or WPI can be further processed with hydrolytic enzymes to produce whey protein hydrolysates (WPH) (Foegeding et al., 2011). Whey protein concentrates and isolates share two principal globular proteins,  $\beta$ -lactoglobulin ( $\beta$ -LG) and  $\alpha$ -lactalbumin ( $\alpha$ -LA), in various proportions.

One of the main applications of whey protein ingredients is in functional beverages (Eckert & Riker, 2007; Ozer & Kirmaci, 2010) that can be generally categorized based on pH as being acidic or neutral. This also determines the thermal processing (time and temperature) requirement to comply with product safety and shelf life. Generally, to be considered shelf-stable, a beverage must be commercially sterile and remain a homogeneous sol after thermal processing. Commercially sterile beverages receive a heat treatment, with an increased degree of thermal treatment required for low acid beverages ( $\text{pH} > 4.6$ ) compared with that for the high acid beverages ( $\text{pH} < 4.6$ ) due to the higher microbial growth risk for the former (Title 21, Code of Federal Regulations 113 and 114).

Whey proteins start to denature at temperatures above  $60^\circ\text{C}$ , and the denatured state favors aggregation (Anema & McKenna, 1996; Croguennec, O'Kennedy, & Mehra, 2004; Dissanayake, Ramchandran, Donkor, & Vasiljevic, 2013; Galani & Apenten, 1999; Le Bon, Nicolai, & Durand, 1999; McGuffey, Epting, Kelly, & Foegeding, 2005). The extent of aggregation caused during processing and storage determines shelf life based on undesirable changes in physical properties. Shelf life is terminated when aggregation produces an undesirable increase in viscosity, a visible precipitate or other form of phase separation, or gelation.

\* Corresponding author. Tel.: +1 919 513 2244.

E-mail address: [allen\\_foegeding@ncsu.edu](mailto:allen_foegeding@ncsu.edu) (E.A. Foegeding).<sup>1</sup> Department of Food Technology, Faculty of Engineering, Pasundan University, Bandung-Jabar, Indonesia. Campus IV Jl. Dr. Setiabudhi No. 193 Bandung – West Java, 40153, Indonesia.

In the context of a beverage, protein heat stability can be defined as forming a stable sol with protein particles of a desired size and shape after thermal processing. This differs from the classical perspective of protein structural stability being a measure of loss of biological function due to denaturation. Protein heat stability in beverages is therefore related to the extent of aggregation and has been evaluated by measuring changes in solubility (De Wit, 1990; de Wit & Kessel, 1996; Pelegrine & Gasparetto, 2005) or turbidity (Kinekawa & Kitabatake, 1995; LaClair & Etzel, 2009).

A state diagram representing heat stability of proteins in beverages should show the combination of variables that produce a sol as well as unstable states of precipitate and gel. Ako, Nicolai, Durand, and Brotond (2009) developed a comprehensive state diagram approach based on extensive heating at 80 °C to produce a steady degree of aggregation. The state diagram displayed transitions among colloidal structures of sol, precipitate, homogenous gel, and micro-phase separated gel. However, differences in solubility were not measured within the sol phase. Wagoner, Ward, and Foegeding (2015) used state diagrams to evaluate aspects of colloidal stability of a model WPI beverage after thermal treatment. Thermal stability was shown by state diagrams for protein solubility, turbidity, and colloidal structure as a function of pH and protein concentration. Also, the method of Wagoner et al. (2015) used thermal treatments at > 100 °C to more closely simulate industrial beverage processing.

We hypothesize that the state diagram approach described by Wagoner et al. (2015) can show differences in heat stability among various types of whey protein ingredients. Therefore, the first objective was to use the state diagram approach to identify the heat stability regions for several whey protein ingredients. The variables of pH (3–7) and protein concentration (1–10%, w/w) were chosen to represent ranges that could be found in beverages. The second objective was to compare state diagrams created by short time thermal processes at temperatures >100 °C (Wagoner et al., 2015) with the extensive heating at temperatures < 100 °C to determine if a steady degree of aggregation is achieved under various time–temperature heating conditions.

## 2. Materials and methods

### 2.1. Materials

Commercial whey protein concentrates (WPC), isolates (WPI), and hydrolysates (WPH) were provided by Glanbia Nutritionals (Twin Falls, ID, USA). Protein contents of the whey protein ingredients were determined by Dumas nitrogen analysis using a conversion factor of 6.38 (% protein = % nitrogen × 6.38). Mineral compositions were determined by inductively coupled plasma atomic emission spectroscopy. The manufacturer provided lactose and lipid content. Chemical reagents were of analytical grade and supplied by Sigma–Aldrich (St. Louis, MO, USA).

### 2.2. Sample preparation

A stock solution (12%, w/w, protein) of each whey ingredient was created by solubilizing powders in deionized water (>17 MΩ) by mixing with a magnetic stirrer (400 rpm) for 3 h at 22 ± 2 °C and storing overnight at 5 °C for additional hydration. Solutions were diluted to the appropriate concentration with deionized water, and sodium azide was added at a final concentration of 0.02% (w/w) to limit microbial growth. All pH adjustments were made with a combination of acids commonly used in commercial beverages (65%, v/v, 1 M phosphoric acid, 35%, v/v, 1 M citric acid) or 1 M sodium hydroxide. The volume added during pH adjustment was included in determining final concentration of each protein solution. Protein

concentration ranged from 1 to 10% with 1% increments and pH values ranged from 3 to 7 with 0.5 unit increments.

### 2.3. Thermal processing treatment

#### 2.3.1. Heating at $T > 100$ °C

Thermal processing was conducted following the method described by Wagoner et al. (2015), where two different heat treatments were used to mimic industrial processes based on beverage pH: 109 °C for 3 s when pH ≤ 4.5, and 141 °C for 6 s when pH > 4.5. Sample solutions (2 mL) were placed in capped borosilicate culture tubes (16 × 100 mm) (Thermo Fisher Scientific, Waltham, MA, USA) and equilibrated to room temperature (22 ± 2 °C) before thermal processing. Thermal processing was done in a Neslab EX7 silicon oil bath (Thermo Fisher Scientific) fixed at 150 °C. Tubes were agitated by manually shaking the filled tube rack during heating for total processing times (heating ramp + holding time) of 29 + 3 s and 62 + 6 s for respective thermal processes of 109 °C for 3 s and 141 °C for 6 s (Wagoner et al., 2015). The overall heating time was the initial time required to reach the target temperature of 109 °C (29 s) or 141 °C (62 s), plus 3 or 6 s respectively for a holding time. During holding, the temperature only increased by 0.1–0.3 °C. After heating, the tubes were immersed in an ice slurry for 5 min and then stored overnight at 5 °C before running all analyses.

#### 2.3.2. Heating at $T < 100$ °C

All solutions at pH 3.5, 4, 4.5, 6.5 and 7.0 were heated in a water bath at temperatures of 80, 85, 90, 95, or 99 °C for times ranging from 1 to 16 h. The heated samples were equilibrated at room temperature for 1 h and then held at 5 °C. The colloidal structure was recorded after storing overnight at 5 °C.

### 2.4. Evaluation of the colloidal structure

The colloidal structure was determined by visual inspection. Samples were either single phase and fluid (sol), had a visible precipitate (precipitate), or formed a solid gel that did not flow when the tube was inverted (gel). The colloidal structure (sol, precipitate, or gel) was assigned to a numeric scaling (1 = sol, 2 = precipitated, and 3 = gel) to allow for plotting in the contour map function of Sigma Plot (Systat Software, San Jose, CA, USA).

### 2.5. Turbidity

The measurement of turbidity (i.e., optical clarity) is based on degree of transmission or light-scattering (nephelometry; Kitchener, Wainwright, & Parsons, 2017). Nephelometry was used because it avoids any concern about absorbance and provided a greater dynamic range than transmission. The turbidity values (nephelometric turbidity units; NTU) of the fluid samples after thermal treatment were determined using a HACH 21000AN Turbidimeter (Hach Company, Loveland, CO, USA). Sol and precipitated samples were pipetted into borosilicate disposable plain tubes OD 16 × 100 mm (Thermo Fisher Scientific) and diluted 1:5 (1 part sample and 4 parts deionized water) before the measurement. The dilution factor was accounted for in the reported values. Samples that could not be homogeneously dispersed were indicated as > 5.10<sup>4</sup> NTU. All measurements were made using the complete set of detectors (ratio mode) (HACH, 2006).

### 2.6. Amount of soluble protein

The percentage of soluble protein was calculated as a percentage of the protein concentration of the unheated solution without pH

adjustment. The amount of soluble protein was determined for sol, precipitate and soft-gelled samples, as they all could be dispersed and diluted for analysis. Stiff gels ruptured into gel particles and were not analyzed. Protein dispersions were centrifuged at  $17,200\times g$  for 20 min at 15 °C to remove insoluble particles, per the method of Wagoner et al. (2015). The supernatant was diluted 1:20 with deionized water, and the protein content was determined using the bicinchoninic acid (BCA) Protein Assay Kit according to producer's instructions (Pierce, Rockford, IL, USA). Protein assay reagents were mixed with the protein sample and incubated in 96-well plates at 37 °C for 30 min. The absorbance at 562 nm was determined using a microplate reader (Tecan Safire<sup>2</sup>, Männedorf, Switzerland). A standard curve was developed using serial dilutions of WPI.

### 2.7. Development of state diagrams

State diagrams were constructed based on the procedure and thermal processing conditions described by Wagoner et al. (2015) with a slight modification of the solubility calculation. Protein solubility after thermal processing was represented as a percentage of the solubility of the hydrated whey protein ingredient, before pH adjustment and thermal processing. The percentage of soluble protein that remained dispersed after thermal processing was used as an indication of heat stability. State diagrams were constructed based on percent soluble protein, turbidity, and colloidal structure after thermal processing. Values are the average from three replications. The standard deviations in solubility for areas with high solubility were 0.02–0.07%, while those for those at the sol/precipitate transition were 0.03–0.11%. State diagrams were produced using the contour map function of Sigma Plot (Systat Software). The contour plots were constructed based on a converted xyz triplet data (pH, protein concentration, and turbidity or solubility) to evenly increment the mesh data (SPSS Science Marketing Department, 2002).

#### 2.7.1. Heat stable regions

The region (pH and protein concentration) in the state diagrams that corresponded to  $\geq 80\%$  protein solubility after heating was defined as the heat stable region. The area of the heat stable regions was determined by cutting the area out of the state diagram and then converting the paper weight to area (Ranganna, 1986):

$$\text{Area of heat stable region} = \text{weight (g) of region} \times (\text{standard area/g of paper}) \quad (1)$$

The standard used was a rectangular paper area of 58.06 mm<sup>2</sup> with known weight of 0.048 g. The area values reported were averages from three independent replicates. The paper used was tested for consistency and the weight per unit area of an individual paper sheet was constant over the paper's entire area (data not shown).

### 2.8. Sodium dodecyl sulfate-polyacrylamide gel electrophoresis

Gel electrophoresis (reduced SDS-PAGE) was run on pre- and post-thermal processed protein samples. Samples were centrifuged as described above, and the supernatant was diluted using Phosphate Buffer Saline (PBS) to a protein concentration of 2  $\mu\text{g } \mu\text{L}^{-1}$ . Samples of protein in PBS (40  $\mu\text{L}$ ) were mixed with NuPAGE LDS sample buffer (25  $\mu\text{L}$ ), NuPAGE Reducing agent containing DTT (10  $\mu\text{L}$ ), and 25  $\mu\text{L}$  standard PBS following the instructions for precast Novex NuPAGE Bis-Tris Mini Gels (4–12% acrylamide). The final protein concentration was 0.8  $\mu\text{g } \mu\text{L}^{-1}$  in a total mix of 100  $\mu\text{L}$ . For each gel, 10  $\mu\text{L}$  Novex Sharp pre-stained

protein standard (Life Technologies, Grand Island, NY, USA) was loaded in the first lane, followed by 10  $\mu\text{L}$  (0.8  $\mu\text{g } \mu\text{L}^{-1}$ ) of each sample in the neighboring lanes. All electrophoresis was done using a Novex NuPAGE gel system (Invitrogen Corp., Carlsbad, CA, USA) and NuPAGE MES SDS Running buffer. Antioxidant (Invitrogen Corp.) (500  $\mu\text{L}$ ) was added to the upper chamber running buffer (200 mL volume) to prevent sample re-oxidation and maintain the reduced state of the proteins. Gels were run at 200 V for 35 min. After electrophoresis, gels were rinsed with deionized water and stained using SafeStain Coomassie stain (Invitrogen Corp.) for 60 min and destained with deionized water for 16 h. Gel images were taken, and band intensities were measured using ImageLab software of the GelDoc XR + molecular imager (Bio-Rad Laboratories, Hercules, CA, USA). The band intensities of  $\beta$ -LG,  $\alpha$ -LA, and bovine serum albumin (BSA) were expressed as a percentage of the sum of the intensities of  $\beta$ -LG,  $\alpha$ -LA, and BSA from each lane. Band intensity percentage values reported are average values from two independent replicates.

### 2.9. Nano differential scanning calorimetry

A nano DSC differential scanning calorimeter (N-DSC II, TA Instruments, previously Calorimetry Sciences Corp., Provo, UT, USA) was used to determine peak denaturation temperature ( $T_d$ ) and denaturation enthalpy ( $\Delta H$ ). Protein solutions were adjusted to pH 3.5 or 7 and diluted to 1.5 mg mL<sup>-1</sup> protein. Samples and a reference (deionized water) were degassed at  $\sim 1100$  Torr for 1 h before analysis. Sample and reference volumes of 0.3 mL were inserted into respective sample and reference capillaries. A constant pressure of 3.0 atm was applied and samples were heated from 30 °C to 110 °C at a rate of 1 °C min<sup>-1</sup>. The molar heat capacity values of the protein solutions were corrected by subtracting the values for water. The change in molar heat capacity was analyzed using a polynomial equation to calculate denaturation enthalpy and peak denaturation temperature. Molar denaturation enthalpy was calculated based on the molar mass of  $\beta$ -lactoglobulin.

### 2.10. Statistical analysis

Data are from three independent main process replications unless otherwise stated. Analysis of variance (ANOVA) was performed using JMP 11.0 (SAS, Cary, NC, USA). When experimental factors were found to be significant ( $p < 0.05$ ), differences between means (factor levels) were compared (determined to be significantly different or not) using Tukey's studentized range test to control for Type I Error.

Multivariate correlation coefficients ( $r$ ) were determined using JMP 11.0 with restricted maximum likelihood (REML) as a method for fitting linear mixed models.

## 3. Results

### 3.1. Compositional difference

Trends in protein, carbohydrate, and lipid composition were in accordance with product type; WPI and WPH were higher in protein and lower in carbohydrate and lipids than WPCs (Table 1). Among WPCs, WPC-B had the highest amount of protein followed by WPC-C, WPC-A, and lastly WPC-D.

### 3.2. State diagrams for heating at $T > 100$ °C

The state diagrams depict changes in colloidal structure, heat stability, and turbidity across pH 3 to 7 at protein concentrations ranging from 1 to 10% (w/w). State diagrams were grouped for

**Table 1**  
Composition (% w/w) of the whey protein ingredients (dry weight basis).

Component	WPC-A	WPC-B	WPC-C	WPC-D	WPH	WPI
Protein	74.7	80.4	78.5	73.2	85.0	90.5
Lactose	5.10	4.70	5.70	4.30	1.70	1.40
Lipids	10.9	7.16	6.30	15.0	0.40	0.60
Calcium	0.71	0.36	0.49	0.3	0.54	0.56
Phosphorous	0.78	0.32	0.43	0.42	0.29	0.27
Potassium	0.63	0.47	0.99	0.35	1.81	0.42
Magnesium	0.07	0.06	0.06	0.05	0.11	0.10
Sodium	0.36	0.24	0.27	0.18	0.57	0.23
Sulfur	0.82	0.87	0.92	0.81	1.03	1.05

comparison among the four WPCs (Fig. 1) and WPH and WPI (Fig. 2).

**3.2.1. Colloidal structure comparison among whey protein ingredients**

Three patterns of transitions of colloidal structures with pH were observed that depended on protein concentration (Figs. 1 and 2). At protein concentrations below the critical gelation concentration ( $C_0 \sim 4\%$ , w/w), moving from pH 3 to pH 7 caused transitions from sol  $\rightarrow$  precipitate  $\rightarrow$  sol. As protein concentration increased to intermediate levels, the transition was: sol  $\rightarrow$  precipitate  $\rightarrow$  gel  $\rightarrow$

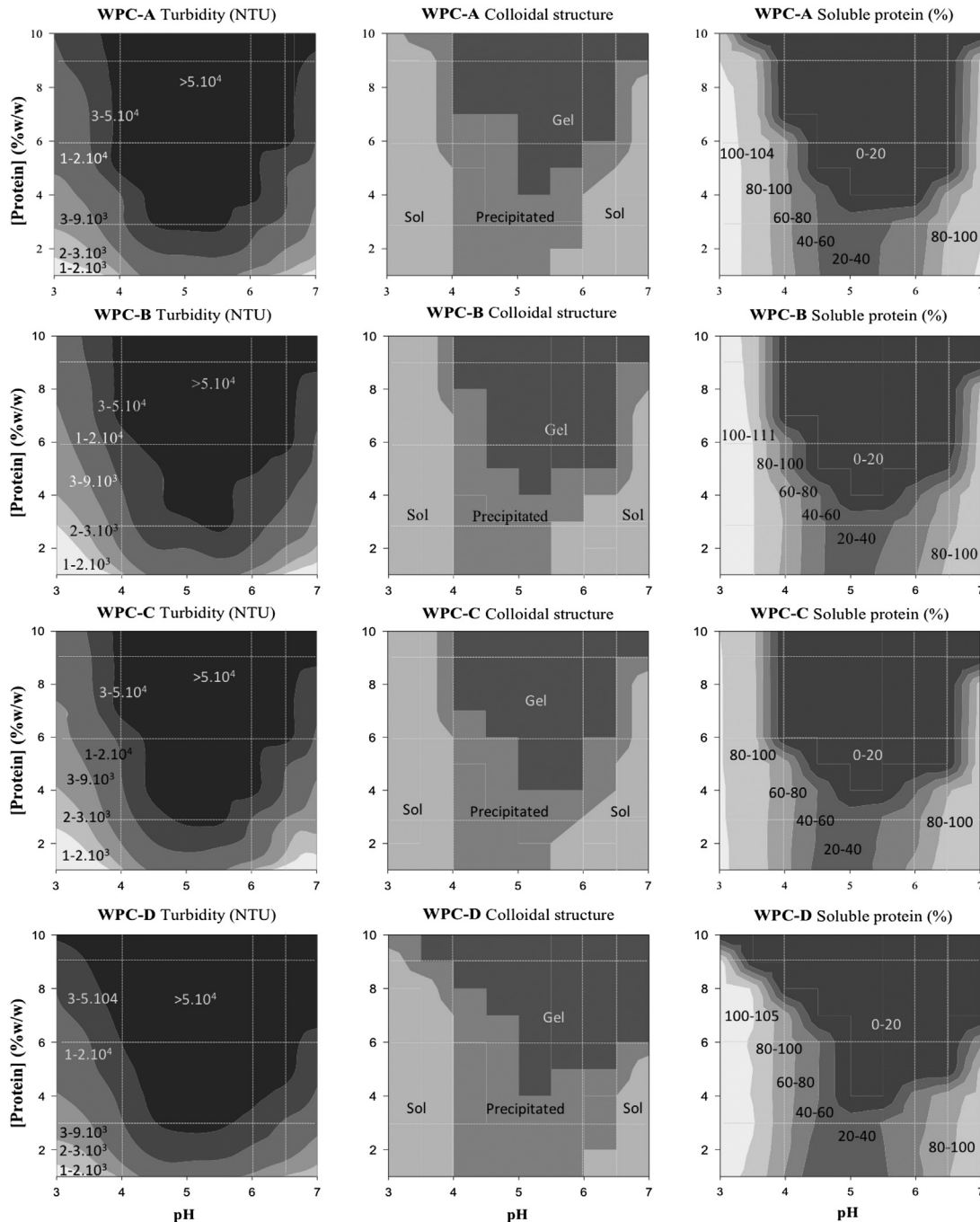


**Fig. 1.** State diagrams for whey protein concentrates. Vertical and horizontal lines were added to aid in comparison among treatments. Numbers in turbidity diagrams are the range of turbidity units (NTU) represented by the area. Colloidal structures diagrams show the structure of sol, precipitate, or gel of the samples for respective treatments. Soluble protein (%) is percentage of soluble protein remaining after thermal processing.

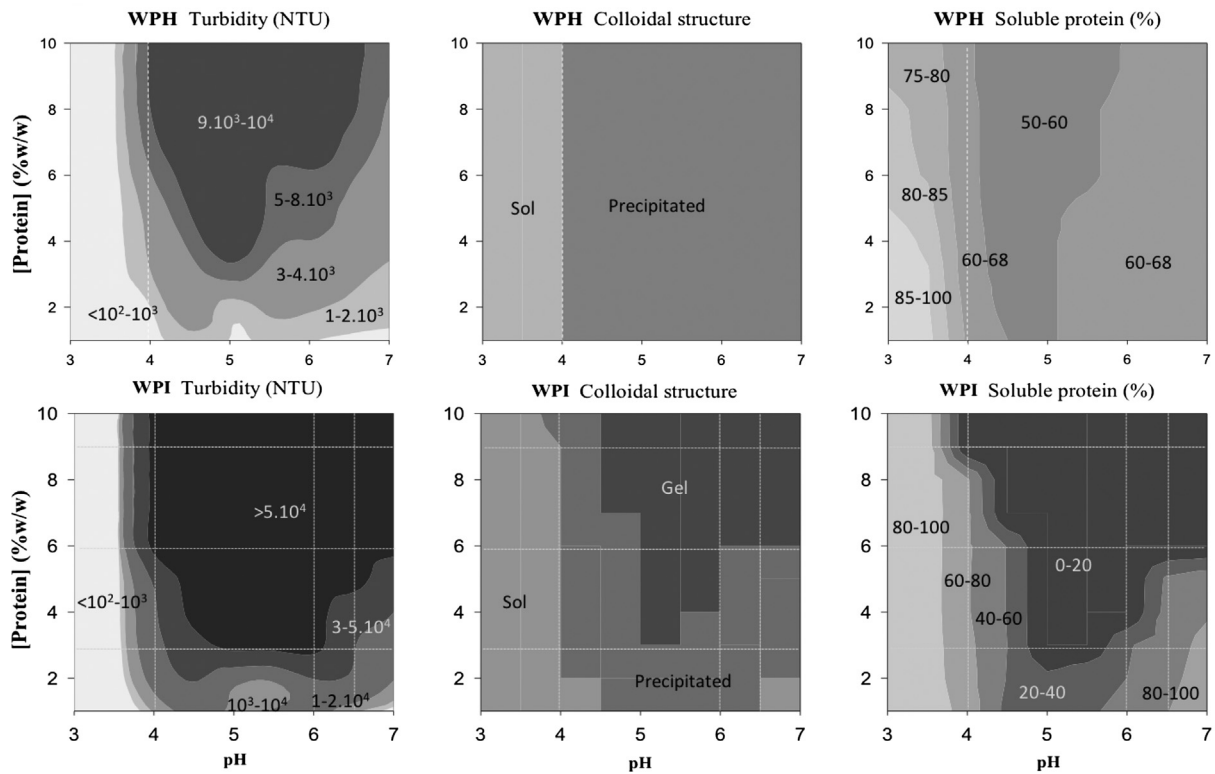


**Fig. 2.** State diagrams for whey protein isolate and whey protein hydrolysate. Numbers in turbidity diagrams are the range of turbidity units (NTU) represented by the area. Colloidal structures diagrams show the structure of sol, precipitate, or gel of the samples for respective treatments. Soluble protein (%) is a percentage of soluble protein remaining after thermal processing.

precipitate → sol. Lastly, at protein concentrations well above  $C_0$  the transition was: sol → precipitate → gel. Colloidal structures at three pH values (pH 3.5, 4.5, and 7.0) were compared based on the protein concentration range that produces the colloidal structure (Table 2). All ingredients had unique patterns for protein concentrations associated with colloidal structures across pH values. For the WPCs, the pH 4.5 region produced the most differences.

### 3.2.2. Turbidity

The turbidity values of all ingredients increased as the pH approached the isoelectric points of whey proteins (pH 4.2–4.5 for  $\alpha$ -lactalbumin and 5.13 for  $\beta$ -LG; Eigel et al., 1984) and increased protein concentration (Figs. 1 and 2). Turbidity increases at a constant refractive index reflect changes in particle size, number, and shape coinciding with increased aggregation caused by lowering electrostatic stabilization (pH change) or increasing protein concentration. The cause of the slightly lower turbidity values for WPI

and WPH around pH 5 was not clear. Among WPCs, it appeared that WPC-A, B, and C shared trend similarities in turbidity and colloidal structure that were different than WPC-D.

### 3.2.3. Percent soluble protein after thermal processing

The most sensitive factor for differentiating the ingredients was the percent soluble protein after heating (Figs. 1 and 2). Calculating the percent soluble protein based on the initial solubility of the unheated protein solution produced some values over 100%, which was due to a combination of several possibilities including slight variability in the assay and increased solubility of the protein powder at low pH. However, this does not change the overall trends in the data. Within the low pH (3–3.5) sol region, all ingredients had the highest percentage of soluble protein and the amount was less dependent on protein concentration (Figs. 1 and 2). Within the higher pH (6.5–7) sol region, the heat stability of WPCs was lower compared with the low pH region. It can also be observed that the

**Table 2**

Patterns in colloidal structures and their associated protein concentration (%) ranges based on state diagrams.

Ingredient	Ranges of protein concentration (%) at								
	pH 3.5			pH 4.5		pH 7			
	Sol	Prec.	Gel	Prec.	Gel	Sol	Prec.	Gel	
WPC-A	1–9	9–10	–	1–7	7–10	1–8	8–9	9–10	
WPC-B	1–10	–	–	1–5	5–10	1–8	8–9	9–10	
WPC-C	1–10	–	–	1–6	6–10	1–8	8–9	9–10	
WPC-D	1–8	8–9	9–10	1–7	7–10	1–5	5–6	6–10	
WPH	1–10	–	–	1–10	–	–	1–10	–	
WPI	1–10	–	–	1–7	7–10	1–2	2–6	6–10	

**Table 3**

The state diagram area representing  $\geq 80\%$  protein solubility in the low and high pH regions.<sup>a</sup>

Ingredient	Area (mm <sup>2</sup> )	
	Low pH	High pH
WPC-A	60.4 ± 0.36 <sup>b</sup>	19.1 ± 0.68 <sup>b</sup>
WPC-B	67.2 ± 1.34 <sup>a</sup>	17.0 ± 0.37 <sup>c</sup>
WPC-C	57.7 ± 0.28 <sup>c</sup>	21.8 ± 0.44 <sup>a</sup>
WPC-D	59.5 ± 0.94 <sup>bc</sup>	12.6 ± 0.19 <sup>d</sup>
WPH	40.2 ± 0.19 <sup>d</sup>	0 <sup>f</sup>
WPI	60.5 ± 0.67 <sup>b</sup>	8.3 ± 0.12 <sup>e</sup>

<sup>a</sup> Values within a column with different letters indicate significant differences ( $p < 0.05$ ).

closer the pH is to the isoelectric points of whey proteins (~pH 4.2–5.2) and the higher the protein concentration, the lower the heat stability; supporting the finding of other investigations (Guyomarc'h, Renan, Chatriot, Gamerre, & Famelart, 2007; Laleye,

Jobe, & Wasesa, 2008; Prazeres, Carvalho, & Rivas, 2012; Ramos et al., 2012; Verheul, Roefs, & de Kruijff, 1998; Wang & Ismail, 2012).

Heat stability regions were defined as the phase diagram area accounting for  $\geq 80\%$  soluble protein. In the low pH range, WPC-B

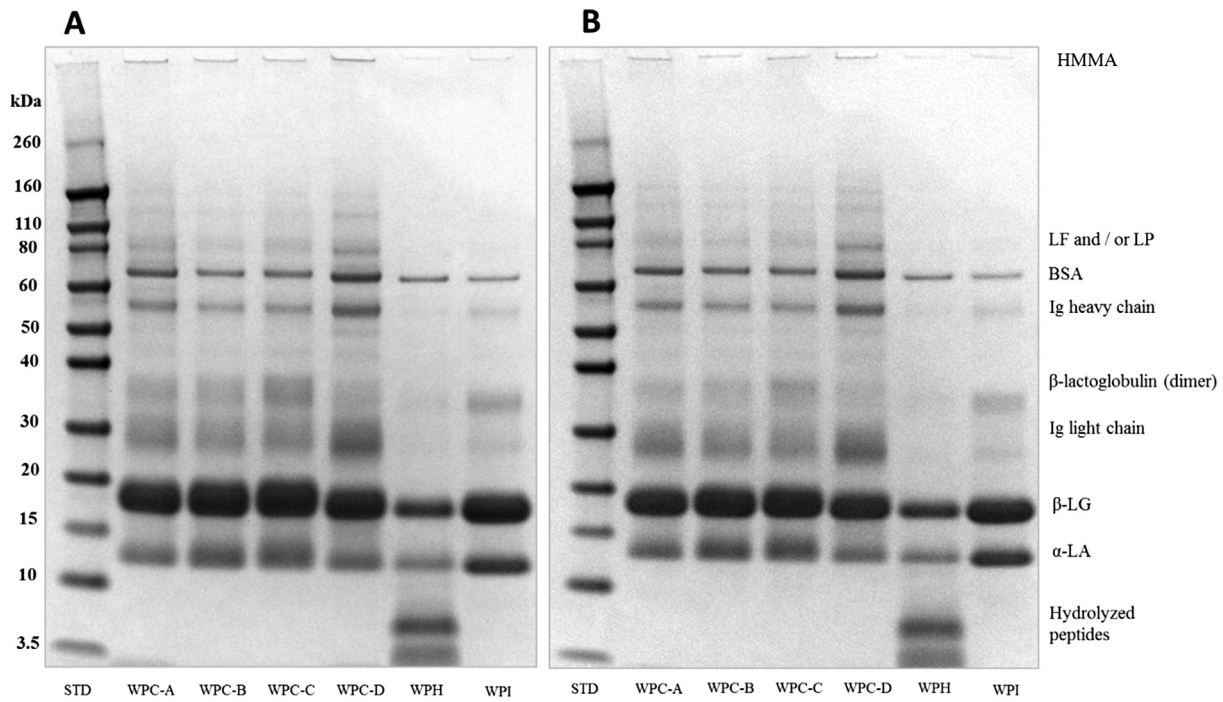


**Fig. 3.** Electrophoretic gel of soluble protein from unheated (A) and heated (B) solutions prepared at pH 3.5 and protein concentration of 8% (w/w). All lanes on both gels were loaded with the same amount of protein. HMMA, high molecular mass aggregates; LF, Lactoferrin, LP, lactoperoxidase; Ig, immunoglobulin;  $\beta$ -LG,  $\beta$ -lactoglobulin;  $\alpha$ -LA,  $\alpha$ -lactalbumin; BSA, bovine serum albumin.

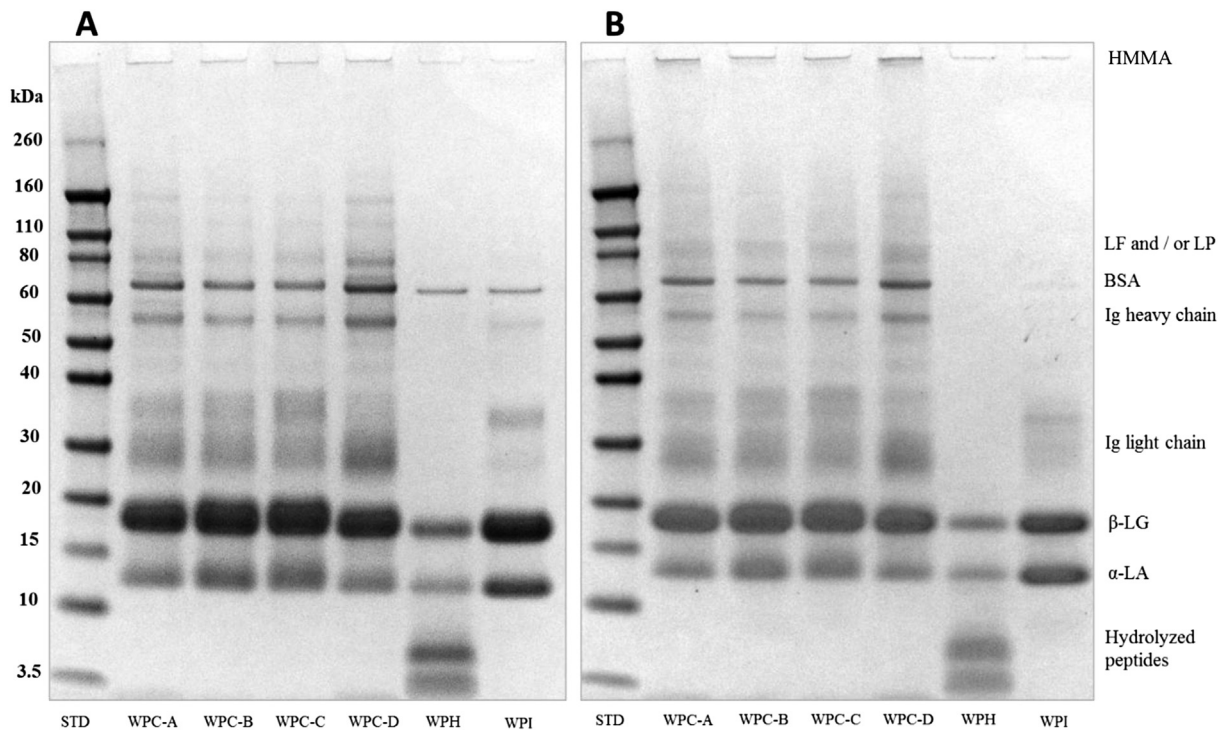


**Fig. 4.** Electrophoretic gel of soluble protein from unheated (A) and heated (B) solutions prepared at pH 7 and protein concentration 5% w/w. All lanes on both gels were loaded with the same amount of protein. HMMA, high molecular mass aggregates; LF, Lactoferrin, LP, lactoperoxidase; Ig, immunoglobulin;  $\beta$ -LG,  $\beta$ -lactoglobulin;  $\alpha$ -LA,  $\alpha$ -lactalbumin; BSA, bovine serum albumin.

had the largest heat stability region and the order from the most stable to the least was: WPC-B > WPC-A ≈ WPI ≈ WPC-D ≈ WPC-C > WPH (Table 3). In the higher pH range, WPC-C was the most stable and the order was: WPC-C > WPC-A > WPC-B > WPC-D > WPI > WPH. Within the higher pH (6.5–7) sol region, the heat stability of WPCs was lower compared with low pH region (3–3.5); however, it should be noted that this is related to differences in not only pH but also heat treatments.

### 3.3. Compositional factors associated with changes in state diagrams

All WPCs had a greater amount of carbohydrates and lipids than WPI and WPH (Table 1). There was no trend observed between non-protein components and state diagrams with the exception of a correlation between sugar percentage in solution and the solubility at 5% w/w protein at pH 7 ( $r = 0.883$ ). Lipid content did not show any overall trends in association with colloidal stability.

The amounts of individual soluble proteins before and after thermal processing were compared. Protein concentrations of 8% and 5% were chosen because they were the highest concentrations at the pH (3.5 and 7, respectively) that produced a sol after thermal processing (Fig. 1). At pH 3.5, there were no perceptible changes in the individual protein bands on electrophoretic gels after the heating process (Fig. 3). This was supported by similar proportion of the relative band intensities ( $\beta$ -LG,  $\alpha$ -LA, and BSA) between the unheated and the heated proteins determined by densitometry (data not shown) and similar amount of soluble protein (Figs. 1 and 2). By comparison, at pH 7 the post-heating relative band intensities (%) of the individual whey proteins were lower than the unheated ones (Fig. 4; Table 4). The approximate percent reduction of the individual proteins ( $\beta$ -LG,  $\alpha$ -LA, and BSA) at pH 7 was the same across all ingredients (no significant difference,  $p > 0.05$ ). The decrease of the band intensities was accompanied by an increase of high molecular mass aggregates (HMMA; >260 kD) that can be seen as accumulated dark strips at the top of the gel, and increase in the HMMA band intensities (Fig. 4 and Table 4).

### 3.4. Thermal properties

Calorimetry was used to see if denaturation temperature ( $T_d$ ) and enthalpy ( $\Delta H$ ) could be used to differentiate the ingredients (Fig. 5). Denaturation temperature was determined as the peak of the endothermic curve, while  $\Delta H$  was determined by analyzing the area between the endothermic curves and baselines. At pH 3.5 there were only slight differences in  $T_d$ , with a range of 90.5 °C for WPI and 91.8 °C for WPH. The WPCs had similar  $\Delta H$  values with the exception of WPC-D being lower (Table 5). The  $\Delta H$  values at pH 7 differed among WPCs with WPC-A having the lowest value. Whey protein isolate had significantly ( $p < 0.05$ ) higher  $\Delta H$  than WPCs and WPH at pH 3.5 and pH 7.0 (Table 5). At pH 7, WPI showed two

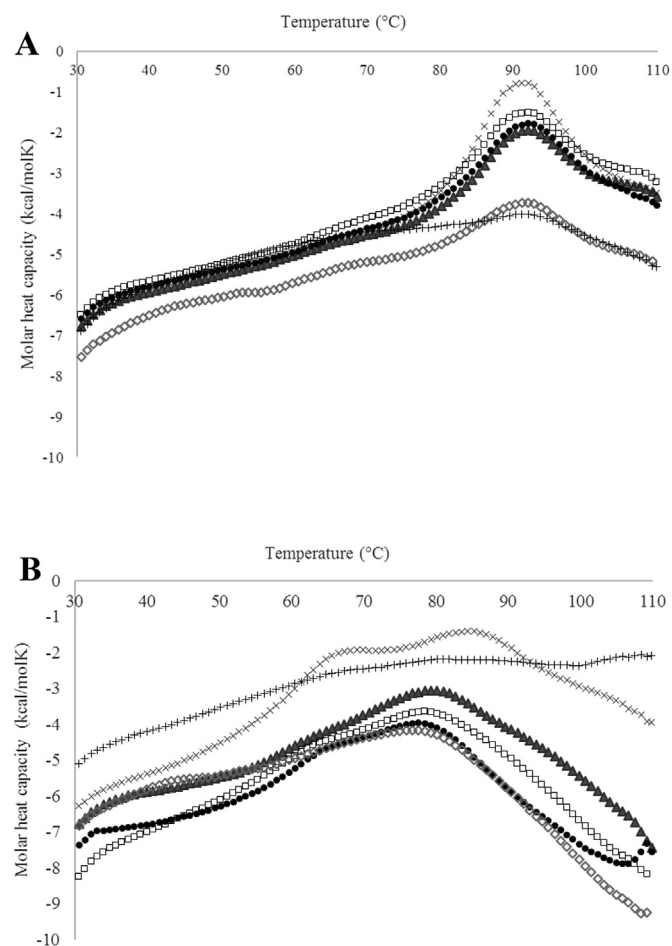


Fig. 5. Molar heat capacity at constant pressure ( $C_p$ ) of 1.5 mg mL<sup>-1</sup> whey protein ingredients at pH 3.5 (A) and 7.0 (B): ▲, WPC-A; □, WPC-B; ●, WPC-C; ◇, WPC-D; +, WPH; ×, WPI. Each point in the curve was averaged from three replicates.

distinctive peaks (Fig. 5B). The other ingredients also showed two peaks, although not as distinctive as WPI. The lower temperature peak corresponded to the denaturation of holo  $\alpha$ -LA, which depending on calcium ion content, varies from 64 to 70 °C (Hendrix, Griko, & Privalov, 2000).

### 3.5. Comparison of model processes ( $T > 100$ °C) and heating at $T < 100$ °C

The state diagrams produced by Ako, Nicolai, Durand, and Brotons (2009) were based on  $\beta$ -LG solutions heated overnight at 80 °C to achieve a steady state (i.e., no change in particle size) of aggregation. In comparison, this investigation used thermal

Table 4  
Electrophoretic bands and intensity differences (%) between soluble protein before and after heating 5% (w/w) solutions at pH 7.<sup>a</sup>

Protein	Intensity difference (%)					
	WPC-A	WPC-B	WPC-C	WPC-D	WPH	WPI
HMMA	1.30 ± 0.42	0.70 ± 0.42	1.30 ± 0.71	2.15 ± 1.91	0.90 ± 0.42	0.80 ± 0.71
BSA	-2.15 ± 0.35	-1.95 ± 1.77	-0.75 ± 0.64	-1.75 ± 0.35	-3.75 ± 0.49	-2.20 ± 0.71
$\beta$ -LG	-6.80 ± 1.98	-7.0 ± 0.42	-4.50 ± 3.25	-5.20 ± 3.39	-2.15 ± 0.64	-7.70 ± 4.95
$\alpha$ -LA	-1.60 ± 1.56	-1.15 ± 0.21	-1.55 ± 1.34	-2.60 ± 0.99	-2.20 ± 1.84	-2.95 ± 1.34

<sup>a</sup> There were no significant differences among values from the same row ( $p > 0.05$ ). All relative band intensities were from electrophoretic gels bands from Fig. 4. HMMA: high molecular mass aggregates, positive values indicate an increase and negative values indicate a decrease in percentage.

**Table 5**  
Enthalpy ( $\Delta H$ ) and denaturation temperature ( $T_d$ ) of whey protein ingredients samples determined through nano differential scanning calorimetry.<sup>a</sup>

pH	Thermal properties	WPC-A	WPC-B	WPC-C	WPC-D	WPH	WPI
3.5	$\Delta H$ (kcal mol <sup>-1</sup> )	17.2 ± 0.8 <sup>b</sup>	17.3 ± 0.6 <sup>b</sup>	17.5 ± 1.1 <sup>b</sup>	12.3 ± 1.1 <sup>c</sup>	5.96 ± 1.4 <sup>d</sup>	27.1 ± 2.3 <sup>a</sup>
	$T_d$ (°C)	90.6 ± 0.2 <sup>b</sup>	90.7 ± 0.3 <sup>b</sup>	91.3 ± 0.8 <sup>ab</sup>	91.2 ± 0.7 <sup>ab</sup>	91.8 ± 0.2 <sup>a</sup>	90.5 ± 0.1 <sup>b</sup>
7	$\Delta H$ (kcal mol <sup>-1</sup> )	29.5 ± 4.5 <sup>d</sup>	38.9 ± 6.1 <sup>bc</sup>	47.2 ± 6.8 <sup>ab</sup>	34.7 ± 3.2 <sup>cd</sup>	10.9 ± 1.4 <sup>e</sup>	50.8 ± 6.6 <sup>a</sup>
	$T_d$ (°C)	78.7 ± 1.2 <sup>b</sup>	79.6 ± 2.2 <sup>b</sup>	78.9 ± 2.5 <sup>b</sup>	78.0 ± 1.3 <sup>b</sup>	78.3 ± 1.3 <sup>b</sup>	82.7 ± 0.3 <sup>a</sup>

<sup>a</sup> Values within a row with different letters indicate significant differences ( $p < 0.05$ ).

processes that were similar in time–temperature combinations to those used in producing commercial protein-containing beverages. Thermal processes at temperatures <100 °C were investigated to determine if they produce state diagrams similar to those generated at temperatures >100 °C. The colloidal structure was evaluated after thermal processing 8% solutions at pH 3.5, or 6% solutions at pH 4.0, 4.5, 6.5, and 7.0 for various times and several temperatures below 100 °C. These conditions were chosen because, based on

**Table 6**  
Comparison of the colloidal states of heat induced suspension of whey protein ingredients (pH 3.5) that were heated using  $T > 100$  °C versus  $T < 100$  °C processes.<sup>a</sup>

Ingredient (8%, w/w)	$T > 100$ °C		$T < 100$ °C	
	109 °C, 3 s	80 °C, 1 h	80 °C, 2 h	80 °C, 6 h
WPC-A	sol	sgel	sgel	sgel
WPC-B	prec	sgel	sgel	sgel
WPC-C	sol	sgel	sgel	sgel
WPC-D	prec	sgel	sgel	sgel
WPH	prec	sol	sol	sol
WPI	gel	gel	gel	gel

<sup>a</sup> Abbreviations are: sol, homogenous colloidal suspension; prec, precipitated; sgel, soft-gel; gel, stiff-gel.

**Table 7**  
Comparison of the colloidal states of heat induced suspension of whey protein ingredients (pH 4.0 and 4.5) that were heated using  $T > 100$  °C versus  $T < 100$  °C processes.<sup>a</sup>

Ingredient (6%, w/w)	$T > 100$ °C		$T < 100$ °C								
	109 °C, 3 s		80 °C, 2 h		85 °C, 1 h		90 °C, 1 h		95 °C, 1 h		
	pH 4.0	pH 4.5	pH 4.0	pH 4.5	pH 4.0	pH 4.5	pH 4.0	pH 4.5	pH 4.0	pH 4.5	
WPC-A	prec	prec	sgel	sgel	sgel	sgel	sgel	sgel	sgel	sgel	sgel
WPC-B	prec	prec	sgel	sgel	sgel	sgel	sgel	sgel	sgel	sgel	sgel
WPC-C	prec	prec	sgel	sgel	sgel	sgel	sgel	sgel	sgel	sgel	sgel
WPC-D	prec	prec	sgel	sgel	sgel	sgel	sgel	sgel	sgel	sgel	sgel
WPH	prec	prec	prec	prec	prec	prec	prec	prec	prec	prec	prec
WPI	gel	gel	gel	gel	gel	gel	gel	gel	gel	gel	gel

<sup>a</sup> Abbreviations are: sol, homogenous colloidal suspension; prec, precipitated; sgel, soft-gel; gel, stiff-gel.

**Table 8**  
Comparison of the colloidal states of heat-induced suspension of whey protein ingredients (pH 6.5 and 7.0) that were heated using  $T > 100$  °C versus  $T < 100$  °C processes.<sup>a</sup>

Ingredient (6%, w/w)	$T > 100$ °C		$T < 100$ °C											
	140 °C, 6 s		80 °C, 16 h		85 °C, 8 h		90 °C, 8 h		90 °C, 16 h		95 °C, 4 h		99 °C, 3 h	
	pH 6.5	pH 7	pH 6.5	pH 7	pH 6.5	pH 7	pH 6.5	pH 7	pH 6.5	pH 7	pH 6.5	pH 7	pH 6.5	pH 7
WPC-A	sgel	prec	solb	solb	sol	sol	sol	solb	solb	solb	sol	sol	sgel	prec
WPC-B	sgel	prec	solb	solb	sol	sol	sol	sol	solb	solb	prec	sol	sgel	prec
WPC-C	sgel	prec	solb	solb	sol	sol	sol	solb	solb	solb	sol	sol	sol	sol
WPC-D	sgel	prec	solb	solb	sol	sol	sol	sol	solb	solb	prec	sol	sgel	prec
WPH	prec	prec	prec	prec	prec	prec	prec	prec	prec	prec	gel	prec	prec	prec
WPI	gel	gel	gel	sol	gel	sol	gel	sol	gel	sol	gel	prec	gel	gel

<sup>a</sup> Abbreviations are: sol, homogenous colloidal suspension; solb, homogenous colloidal suspension, browned; prec, precipitated; sgel, soft-gel; gel, stiff-gel.

state diagrams, they were the critical conditions where the solutions started to produce varied colloidal structures (sol, precipitate, or gel). For brevity, the thermal processes used in establishing state diagrams will be referred to as  $T > 100$  °C processes.

At pH 3.5, heating WPCs for as little as 1 h at 80 °C produced gels; a sol (WPC-A and C) or precipitate (WPC-B and D) was observed with  $T > 100$  °C processes (Table 6). In contrast, heating WPH at 80 °C (1–6 h) at pH 3.5 produced a sol when a precipitate was observed at  $T > 100$  °C heating. At pH 4.0 and 4.5, the lower temperature/longer heating times resulted in gels in WPCs that had a precipitate under  $T > 100$  °C processes (Table 7). Heating 6% WPI at pH 3.5, 4, and 4.5 at temperatures above and below 100 °C produced gels (Tables 6 and 7).

At pH 6.5 and 7, the effect of heating temperature and time became more apparent. At 80 °C–95 °C, a sol was formed under most conditions except for a gel formed at pH 6.5 with WPI (Table 8). Longer heating times produced browning in WPCs, indicating a greater extent of Maillard browning than in  $T > 100$  °C processes. The 99 °C for 3 h process produced colloidal structures that were similar to the  $T > 100$  °C processes, except for WPC-C, which remained a sol at both pH 6.5 and 7 (Table 8). Overall, no  $T < 100$  °C process produced a state diagram that was similar to the  $T > 100$  °C processes.

## 4. Discussion

### 4.1. State diagram comparison

State diagrams provide information on how a specific set of conditions alter states of a given property. In this case, properties of colloidal structure, appearance (turbidity), and amount of soluble protein were examined as pH and protein content were varied and subjected to thermal processes similar to those used in manufacturing protein beverages. In the context of beverages, this established pH and protein content boundary conditions that resulted in a fluid sol; a minimal requirement for beverage applications of the ingredients.

Two approaches were used to compare state diagrams among ingredients. First, the range of protein concentrations associated with specific colloidal structures at pH 3.5, 4.5, and 7 were compared. This produced protein concentration patterns that were distinct for each ingredient (Table 2). Secondly, heat stability was operationally defined as the area of the state diagram that had  $\geq 80\%$  soluble protein after thermal processing. This produced different patterns for the low ( $< \text{pH } 4.5$ ) and high ( $> \text{pH } 4.5$ ) ranges (Table 3). In the low pH range, the order from the most stable to the least was: WPC-B  $>$  WPI  $\approx$  WPC-A  $\approx$  WPC-D  $\approx$  WPC-C  $>$  WPH. In contrast, in the high pH range the stability ranking was WPC-C  $>$  WPC-A  $>$  WPC-B  $>$  WPC-D  $>$  WPI  $>$  WPH.

No single property provided all the information needed to evaluate functionality in a beverage. Turbidity is problematic because it reflects a broad range of particle sizes. For example, whey protein concentrates had higher turbidity at pH 3–3.5 compared with WPI and WPH (Figs. 1 and 2) due to the fat content of WPC (Table 1). Nevertheless, the stability of WPC, as indicated by % soluble protein, at the pH range 3–3.5 was comparable or better than WPI (Figs. 1 and 2). This demonstrates that broader insight is gained when measuring all three properties when examining the effects of thermal processing.

### 4.2. Comparison of model thermal processes ( $T > 100^\circ\text{C}$ ) and heating at $T < 100^\circ\text{C}$

Thermal processes at temperatures  $< 100^\circ\text{C}$  were investigated to determine if they produced state diagrams similar to those generated at temperatures  $> 100^\circ\text{C}$  (using  $109^\circ\text{C}$  for 3 s and  $141^\circ\text{C}$  for 6 s thermal processes). The colloidal structure was evaluated after thermal processing 8% solutions at pH 3.5, or 6% solutions at pH 4.0, 4.5, 6.5, and 7.0 for various times and temperatures  $< 100^\circ\text{C}$ . The conditions picked were those that started to produce colloidal structures of precipitates and gels (Figs. 1 and 2).

At pH 3.5, 4.0, or 4.5, heating at lower temperature/longer times produced gels in WPCs that had a precipitate under  $T > 100^\circ\text{C}$  processes (Tables 6 and 7). A heat-induced protein gel network is formed when the amount of protein is above a critical minimum concentration ( $C_0$ ) and there is sufficient time for denatured proteins to interact (van der Linden & Foegeding, 2009). The prolonged heating time in the  $T < 100^\circ\text{C}$  treatments allowed for moving from sols or precipitates to gels in all WPCs, indicating that  $109^\circ\text{C}$  for 3 s was insufficient time to establish a gel network. In contrast, gelation was rapid enough in WPI to form a gel network in all pH  $\leq 4.5$  conditions. The  $C_0$  was 4% (w/w) for all WPCs and 3% w/w for WPI (Figs. 1 and 2). This would mean that at 8% w/w protein concentration (C) the  $C/C_0$  would be greater for WPI, and this may explain the faster gelation. An unexpected shift from precipitate to sol in the WPH occurred at pH 3.5, but not at pH 4.0 and 4.5. This cannot be explained based on behavior of intact proteins and requires further investigation.

The results were different at pH 6.5, where heating WPCs at 85, 90, or  $95^\circ\text{C}$  for 8 h or less produced a sol or precipitate, as compared with a soft gel when heated at  $140^\circ\text{C}$  for 6 s (Table 8). This suggests that structural transitions, rather than time limitations, were different when comparing heating at  $140^\circ\text{C}$  to 85–95  $^\circ\text{C}$ . Furthermore, longer heating times (16 h) produced browning in WPCs due to their lactose content. As with results for WPI at pH 3.5, 4, and 4.5 (Tables 6 and 7), the colloidal state of heated WPI is less sensitive to heating time–temperature combinations at pH 6.5. The conditions that most closely resembled the  $140^\circ\text{C}$  for 6 s thermal process were heating at pH 6.5 or 7.0 at  $99^\circ\text{C}$  for 3 h (Table 8). The only exception was WPC-C, which remained a sol at both pH 6.5 and 7 (Table 8). In comparing results for WPCs versus WPI, it appears the non-protein components (lipids, sugars, minerals, and possibly other compounds) are involved in determining colloidal states produced under various thermal processing conditions. These results establish the importance of heat treatment selection when determining a state diagram. If the goal is to generate state diagrams relevant to a beverage application, then the thermal processing conditions must be matched as closely as possible.

### 4.3. Factors associated with heat stability

#### 4.3.1. Compositional properties

There was a positive correlation between the lactose content of the ingredient and % soluble protein after thermal processing at 5% (w/w) and pH 7 ( $r = 0.883$ ). Furthermore, a ranking of heat stability regions at high pH (Table 3) directly follows lactose concentration (Table 1), with an also high correlation coefficient ( $r = 0.91$ ). Proteins are stabilized in an aqueous system that contains sugars, because sugars tend to maintain or increase the hydration of the protein molecule (Arakawa & Timasheff, 1982; Bechtle & Claydon, 1971; Bull & Breese, 1978). However, the correlation between heat stability regions and lactose at pH 3.5 has a low correlation coefficient ( $r = 0.51$ ). This suggests that stability may be more associated with the Maillard reaction, which would be favored at higher pH and heating times, than the effect of sugars on molecular hydration.

Changes in the amount of individual proteins remaining soluble after thermal processing differed due to pH-heat process. At pH 3.5, there were no perceptible changes in the individual protein after the heating process (Fig. 3), supporting the general concept that whey proteins were not significantly affected by the heat process at pH 3.0 or 3.5. Also, at pH 7, there were similar decreases in  $\beta$ -LG,  $\alpha$ -LA, and BSA, and increases in high molecular weight aggregates in all ingredients (Table 4).

#### 4.3.2. Thermal properties

The denaturation temperature,  $T_d$ , is dependent on pH for individual whey proteins (Bernal & Jelen, 1985) and generally increases with a decrease in pH from 7.0 to 3.5 (de Wit & Klarenbeek, 1981; Fitzsimons, Mulvihill, & Morris, 2007; McGuffey et al., 2005). Denaturation temperature was an average of  $91^\circ\text{C}$  at pH 3.5 and  $79.4^\circ\text{C}$  at pH 7  $^\circ\text{C}$  (Table 5). This resulted in a  $\Delta T$  between the heating process and  $T_d$  of  $18^\circ\text{C}$  and  $60.6^\circ\text{C}$  for pH 3.5 and 7.0, respectively. A greater  $\Delta T$  between the heating process and  $T_d$  may cause a greater extent of unfolding, creating different structures. Thus, the heat process for pH 7.0 ( $141^\circ\text{C}$ ) will favor more whey protein aggregates than the heat process used for pH 3.5 ( $109^\circ\text{C}$ ). The whey protein denaturation rate is determined by the heating temperature (Anema & McKenna, 1996; de la Fuente, Singh, & Hemar, 2002; deWit & Klarenbeek, 1984; Iametti, Cairolì, De Gregori, & Bonomi, 1995; Spiegel, 1999). A porous aggregate structure due to a combination of reversible and irreversible aggregation occurs below

90 °C, aggregates become more compact at 90–100 °C, and the temperature range above 100 °C produces dense, compact, and rigid aggregate structures due to rapid unfolding allowing for every collision to produce aggregation (Spiegel, 1999).

A lower relative  $\Delta H$  indicates a higher amount of initial denatured/aggregated protein in the ingredient, assuming a similar protein composition among samples. That could explain WPC-D having the lowest  $\Delta H$  and lower thermal stability at low pH (Tables 3 and 5). However, this is an over simplification because  $\Delta H$  values represent the sum of endothermic (denaturation) and exothermic (aggregation) reactions, so a simple molecular explanation is not possible.

Several thermograms for protein solutions at higher pH had two distinctive peaks, with the most evident seen in WPI at pH 7 (Fig. 5). The lower temperature peak corresponded to the denaturation of  $\alpha$ -LA, which depending on calcium ion content, varies from 64 to 70 °C (Hendrix et al., 2000). At pH 3.5 this lower peak of  $\alpha$ -LA was not observed. This can be explained by disassociation of calcium from the  $\alpha$ -LA structure at low pH causing  $\alpha$ -LA to change conformation from the holo to the apo state, with denaturation temperature around 27 °C (Hendrix et al., 2000). Whey protein concentrates also showed a lower temperature denaturation peak, albeit less than WPI.

#### 4.3.3. Comparison of ingredient properties with state diagrams

Whey protein ingredients and protein containing beverages will also include non-protein components such salts, sugars, lipid, and polyphenols that will alter protein denaturation and aggregation (Anema & McKenna, 1996; de la Fuente et al., 2002; Spiegel, 1999). While non-protein component effects are measurable and usually explained when studied individually, their combined effects are more problematic. This was observed with longer heating time (16 h) of WPC solutions causing observable Maillard browning, while no color was seen in WPI solutions. State diagrams represent the sum of all reactions driving protein aggregation and thereby allow for establishing boundary conditions for a given set of ingredient and processing parameters.

## 5. Conclusions

All six whey protein ingredients produced state diagrams with unique patterns. One differentiating factor was the protein concentrations associated with colloidal structures across pH values, with pH 4.5 showing the greatest differences among ingredients. The second was the size of heat stability regions, defined as the phase diagram area accounting for  $\geq 80\%$  soluble protein. Relative heat stability among ingredients depended on the pH-thermal processing combination, in that patterns observed at pH  $\leq 4.5$  were not equivalent to patterns produced at pH  $> 4.5$ . The most stable ingredient at pH  $< 4.5$  was WPC-B while at pH  $> 4.5$  the most stable ingredient was WPC-C. Heating at temperatures of  $< 100$  °C for extended time did not produce the same results as heating at  $> 100$  °C short times. Therefore, the thermal process used to establish state diagrams must reflect the temperature–time combination that is used in the manufacturing process.

## Acknowledgement

Support from the North Carolina Agricultural Research Service, Glanbia Nutritionals, and Fulbright scholarship are gratefully acknowledged. The use of trade names in this publication does not imply endorsement by the North Carolina Agricultural Research Service of the products named nor criticism of similar ones not mentioned. The authors are very grateful for the whey proteins donated by Glanbia Nutritionals.

## References

- Ako, K., Nicolai, T., Durand, D., & Brotons, G. (2009). Micro-phase separation explains the abrupt structural change of denatured globular protein gels on varying the ionic strength or the pH. *Soft Matter*, 5, 4033.
- Anema, S., & McKenna, A. (1996). Reaction kinetics of thermal denaturation of whey proteins in heated reconstituted whole milk. *Journal of Agricultural and Food Chemistry*, 44, 422–428.
- Arakawa, T., & Timasheff, S. N. (1982). Stabilization of protein structure by sugars. *Biochemistry*, 21, 6536–6544.
- Bechtel, R. M., & Claydon, T. J. (1971). Glucose-residue polymers as protectants against heat denaturation of whey proteins. *Journal of Dairy Science*, 54, 1410–1416.
- Bernal, V., & Jelen, P. (1985). Thermal stability of whey proteins – a calorimetric study. *Journal of Dairy Science*, 68, 2847–2852.
- Blomstrand, E., Eliasson, J., Karlsson, H. K. R., & Kohnke, R. (2006). Branched-chain amino acids activate key enzymes in protein synthesis after physical exercise. *Journal of Nutrition*, 136, 269S–273S.
- Bull, H. B., & Breese, K. (1978). Interaction of alcohols with proteins. *Biopolymers*, 17, 2121–2131.
- Croguenne, T., O'Kennedy, B. T., & Mehra, R. (2004). Heat-induced denaturation/aggregation of  $\beta$ -lactoglobulin A and B: Kinetics of the first intermediates formed. *International Dairy Journal*, 14, 399–409.
- de la Fuente, M. A., Singh, H., & Hemar, Y. (2002). Recent advances in the characterisation of heat-induced aggregates and intermediates of whey proteins. *Trends in Food Science & Technology*, 13, 262–274.
- De Wit, J. N. (1990). Thermal stability and functionality of whey proteins. *Journal of Dairy Science*, 73, 3602–3612.
- de Wit, J. N., & Kessel, T. va (1996). Effects of ionic strength on the solubility of whey protein products. A colloid chemical approach. *Food Hydrocolloids*, 10, 143–149.
- de Wit, J. N., & Klarenbeek, G. (1981). A differential scanning calorimetric study of the thermal behaviour of bovine  $\beta$ -lactoglobulin at temperatures up to 160 °C. *Journal of Dairy Research*, 48, 293–302.
- deWit, J. N., & Klarenbeek, G. (1984). Effects of various heat treatments on structure and solubility of whey proteins. *Journal of Dairy Science*, 67, 2701–2710.
- Dissanayake, M., Ramchandran, L., Donkor, O. N., & Vasiljevic, T. (2013). Denaturation of whey proteins as a function of heat, pH and protein concentration. *International Dairy Journal*, 31, 93–99.
- Eckert, M., & Riker, P. (2007). Overcoming challenges in functional beverages. *Food Technology*, 61, 20–26.
- Eigel, W. N., Butler, J. E., Ernstrom, C. A., Farrell, H. M., Jr., Harwalkar, V. R., Jenness, R., et al. (1984). Nomenclature of proteins of cow's milk: Fifth revision. *Journal of Dairy Science*, 67, 1599–1631.
- Fitzsimons, S. M., Mulvihill, D. M., & Morris, E. R. (2007). Denaturation and aggregation processes in thermal gelation of whey proteins resolved by differential scanning calorimetry. *Food Hydrocolloids*, 21, 638–644.
- Foegeding, E. A., Luck, P., & Vardhanabhuti, B. (2011). Whey protein products. In J. Fuquay, P. Fox, & P. McSweeney (Eds.), *The encyclopedia of dairy sciences*. Oxford, UK: Academic Press.
- Galani, D., & Apenten, R. K. O. (1999). Heat-induced denaturation and aggregation of  $\beta$ -lactoglobulin: Kinetics of formation of hydrophobic and disulphide-linked aggregates. *International Journal of Food Science and Technology*, 34, 467–476.
- Guyomarc'h, F., Renan, M., Chatriot, M., Gamarre, V., & Famelart, M.-H. (2007). Acid gelation properties of heated skim milk as a result of enzymatically induced changes in the micelle/serum distribution of the whey protein/kappa-casein aggregates. *Journal of Agricultural and Food Chemistry*, 55, 10986–10993.
- HACH. (2006). *Turbidimeter model 2100AN* hach.
- Ha, E., & Zemel, M. B. (2003). Functional properties of whey, whey components, and essential amino acids: Mechanisms underlying health benefits for active people (review). *Journal of Nutritional Biochemistry*, 14, 251–258.
- Hendrix, T., Griko, Y. V., & Privalov, P. L. (2000). A calorimetric study of the influence of calcium on the stability of bovine alpha-lactalbumin. *Biophysical Chemistry*, 84, 27–34.
- Hoffman, J. R., & Falvo, M. J. (2004). Protein - which is best? *Journal of Sports Science and Medicine*, 3, 118–130.
- Hulmi, J. J., Laakso, M., Mero, A. A., Häkkinen, K., Ahtiainen, J. P., & Peltonen, H. (2015). The effects of whey protein with or without carbohydrates on resistance training adaptations. *Journal of the International Society of Sports Nutrition*, 12, 1–13.
- Iametti, S., Cairolì, S., De Gregori, B., & Bonomi, F. (1995). Modifications of high-order structures upon heating of  $\beta$ -lactoglobulin: Dependence on the protein concentration. *Journal of Agricultural and Food Chemistry*, 43, 53–58.
- Jakubowicz, D., & Froy, O. (2013). Biochemical and metabolic mechanisms by which dietary whey protein may combat obesity and Type 2 diabetes. *Journal of Nutritional Biochemistry*, 24, 1–5.
- Katsanos, C. S., Chinkes, D. L., Paddon-Jones, D., Zhang, X.-J., Aarsland, A., & Wolfe, R. R. (2008). Whey protein ingestion in elderly persons results in greater muscle protein accrual than ingestion of its constituent essential amino acid content. *Nutrition Research*, 28, 651–658.
- Kawase, M., Hashimoto, H., Hosoda, M., Morita, H., & Hosono, A. (2000). Effect of administration of fermented milk containing whey protein concentrate to rats and healthy men on serum lipids and blood pressure. *Journal of Dairy Science*, 83, 255–263.

- Kimball, S. R., & Jefferson, L. S. (2006). Signaling pathways and molecular mechanisms through which branched-chain amino acids mediate translational control of protein synthesis. *Journal of Nutrition*, 136, 227S–231S.
- Kinekawa, Y., & Kitabatake, N. (1995). Turbidity and rheological properties of gels and sols prepared by heating process whey protein. *Bioscience, Biotechnology and Biochemistry*, 59, 834–840.
- Kitchener, B. G. B., Wainwright, J., & Parsons, A. J. (2017). A review of the principles of turbidity measurement. *Progress in Physical Geography*, 41, 620–642.
- LaClair, C. E., & Etzel, M. R. (2009). Turbidity and protein aggregation in whey protein beverages. *Journal of Food Science*, 74, C526–C535.
- Laleye, L. C., Jobe, B., & Wasesa, A. A. H. (2008). Comparative study on heat stability and functionality of camel and bovine milk whey proteins. *Journal of Dairy Science*, 91, 4527–4534.
- Le Bon, C., Nicolai, T., & Durand, D. (1999). Kinetics of aggregation and gelation of globular proteins after heat-induced denaturation. *Macromolecules*, 32, 6120–6127.
- van der Linden, E., & Foegeding, E. A. (2009). Gelation. Principles, models and applications to proteins. In S. Kasapis, I. T. Norton, & J. B. Ubbink (Eds.), *Modern biopolymer science (1st edn., Chapt. 2)* (pp. 29–91). Oxford, UK: Academic Press.
- Luhovyy, B. L., Akhavan, T., & Anderson, G. H. (2007). Whey proteins in the regulation of food intake and satiety. *Journal of the American College of Nutrition*, 26, 704S–712S.
- Markus, C. R., Olivier, B., Panhuysen, G. E. M., Van Der Gugten, J., Alles, M. S., Tuiten, A., et al. (2000). The bovine protein  $\alpha$ -lactalbumin increases the plasma ratio of tryptophan to the other large neutral amino acids, and in vulnerable subjects raises brain serotonin activity, reduces cortisol concentration, and improves mood under stress. *American Journal of Clinical Nutrition*, 71, 1536–1544.
- McGuffey, M. K., Epting, K. L., Kelly, R. M., & Foegeding, E. A. (2005). Denaturation and aggregation of three  $\alpha$ -lactalbumin preparations at neutral pH. *Journal of Agricultural and Food Chemistry*, 53, 3182–3190.
- Ozer, B., & Kirmaci, H. A. (2010). Quality attributes of yoghurt and functional dairy products. In F. Yildiz (Ed.), *Development and manufacture of yogurt and other functional dairy Products Chapt. 8* (pp. 229–265). Boca Raton, FL, USA: CRC Press.
- Paddon-Jones, D., Campbell, W. W., Jacques, P. F., Kritchevsky, S. B., Moore, L. L., Rodriguez, N. R., et al. (2015). Protein and healthy aging. *American Journal of Clinical Nutrition*, 101, 1339S–1345S.
- Pal, S., & Ellis, V. (2010). The chronic effects of whey proteins on blood pressure, vascular function, and inflammatory markers in overweight individuals. *Obesity*, 18, 1354–1359.
- Pelegrine, D. H. G., & Gasparetto, C. A. (2005). Whey proteins solubility as function of temperature and pH. *LWT - Food Science and Technology*, 38, 77–80.
- Phillips, S. M., Chevalier, S., & Leidy, H. J. (2016). Protein “requirements” beyond the RDA: Implications for optimizing health. *Applied Physiology Nutrition and Metabolism*, 41, 565–572.
- Prazeres, A. R., Carvalho, F., & Rivas, J. (2012). Cheese whey management: A review. *Journal of Environmental Management*, 110, 48–68.
- Ramos, Ó. L., Pereira, J. O., Silva, S. I., Amorim, M. M., Fernandes, J. C., Lopes-da-Silva, J. A., et al. (2012). Effect of composition of commercial whey protein preparations upon gelation at various pH values. *Food Research International*, 48, 681–689.
- Ranganna, S. (1986). *Handbook of analysis and quality control for fruit and vegetable products* (2<sup>nd</sup> ed., p. 775). New Delhi, India: Tata McGraw-Hill Publishing Company Limited.
- Spiegel, T. (1999). Whey protein aggregation under shear conditions - effects of lactose and heating temperature on aggregate size and structure. *International Journal of Food Science and Technology*, 34, 523–531.
- SPSS Science Marketing Department. (2002). *SigmaPlot 8.0 programming guide* ®. Transform. <https://doi.org/10.1089/152791602321105816>.
- Verheul, M., Roefs, S. P. F. M., & de Kruijff, K. G. (1998). Kinetics of heat-induced aggregation of  $\beta$ -lactoglobulin. *Journal of Agricultural and Food Chemistry*, 46, 896–903.
- Wagoner, T. B., Ward, L., & Foegeding, E. A. (2015). Using state diagrams for predicting colloidal stability of whey protein beverages. *Journal of Agricultural and Food Chemistry*, 63, 4335–4344.
- Wang, Q., & Ismail, B. (2012). Effect of Maillard-induced glycosylation on the nutritional quality, solubility, thermal stability and molecular configuration of whey protein. *International Dairy Journal*, 25, 112–122.